Abdel-Nasser, Mohamed; Mahmoud, Karar; Lehtonen, Matti

Reliable Solar Irradiance Forecasting Approach Based on Choquet Integral and Deep LSTMs

Published in:
IEEE Transactions on Industrial Informatics

DOI:
10.1109/TII.2020.2996235

Published: 01/03/2021

Document Version
Peer-reviewed accepted author manuscript, also known as Final accepted manuscript or Post-print

Please cite the original version:
Abdel-Nasser, M., Mahmoud, K., & Lehtonen, M. (2021). Reliable Solar Irradiance Forecasting Approach Based on Choquet Integral and Deep LSTMs. *IEEE Transactions on Industrial Informatics*, *17*(3), 1873-1881. Article 9097938. https://doi.org/10.1109/TII.2020.2996235

Reliable Solar Irradiance Forecasting Approach Based on Choquet Integral and Deep LSTMs

Mohamed Abdel-Nasser, Karar Mahmoud, and Matti Lehtonen

***Abstract*—The intermittent nature associated with photovoltaic (PV) generation is a challenging problem for the optimal planning and efficient management in smart grids. A reliable forecasting model of solar irradiance can play an essential role in allowing high PV penetrations without degrading the grid performance. For this purpose, most related works either use individual forecasting models or ensemble approaches (e.g., weighted average), ignoring the interaction between the values to be aggregated and thus may worsen the forecasting reliability. Differently, we propose a reliable solar irradiance forecasting method based on long short-term memory (LSTM) models and an aggregation function based on Choquet integral. This novel combination has the following features: 1) LSTM models can achieve accurate predictions because they model the temporal changes in solar irradiance, thanks to their recurrent architecture and memory units, and 2) the Choquet integral can model the interaction between the inputs to be aggregated through a fuzzy measure. This aggregation technique can determine the largest consistency among the conflicting forecasting results, taking advantage of each individual model. To demonstrate the effectiveness of the proposed approach, we compare it with several forecasting methods using six realistic datasets collected from different sites in Finland in which solar irradiance is intermittent. The comparison reveals the high reliability of the proposed forecasting model with different sites and solar profiles.**

***Index Terms*—Photovoltaic; irradiance forecasting; deep LSTM; choquet integral.**

I. Introduction

Solar energy is considered as one of the most promising renewable energy sources that are still requiring further investigations and development. Photovoltaic (PV) systems, concentrated solar power stations, and solar water heating are possible technologies to harness solar energy. Indeed, PV systems with their modular and flexible structure are a preferable configuration that can be allocated in the various levels in power systems, including transmission systems, and medium voltage and low voltage distribution feeders [1]–[3]. As the cost of PV systems is declining, their penetrations are continuously expanding. PV systems could have strong positive impacts from the technical and environmental respective. However, their generations have high daily periodicity and seasonal fluctuations as they mainly depend on the highly fluctuated solar irradiance [4]. These characteristics can lead to considerable challenges for integrating large-scale PV farms in transmission systems and an excessive number of distributed PV units in distribution systems. Therefore, reliable forecasting of solar irradiance is of great importance for properly allocating and sizing PV and optimal managing existing PV stations.

In the literature review, several methods are available for solar irradiance forecasting of PV systems. We can categorize them into physical, statistical, persistence, and hybrid approaches. To build the forecasting model, most of these forecasting methods have used mainly historical data of irradiance, as it is the most dominant factor that affects PV generation. In [5], [6], several techniques are introduced to forecast PV irradiance/power for high PV penetrated power systems, as well as smart grid energy management strategies. In [7], various machine learning algorithms, including (1) adaptive network-based fuzzy, (2) auto-regressive integrated moving average (ARIMA), and (3) k-nearest neighbor (KNN) search algorithm have been employed for constructing a numerical based solar irradiance prediction model. The authors of [8] have presented a hybrid forecasting model for global solar irradiance based on the extreme machine learning method and the coral reefs optimizer.

Besides, random forests and artificial neural networks are applied in [9] for forecasting normal beam, horizontal diffuse, and global components of solar irradiance. In [10], a multi-stage multi-variate empirical mode decomposition integrated with the ant-colony optimizer and random forest, have been employed for forecasting monthly solar irradiance. In [11], [12], quantile regression algorithms have been utilized for short-term irradiance forecasting with a resolution of 5 min. In [13], fuzzy logic has been employed to consider the uncertainty of solar irradiance. The authors of [14] have integrated fuzzy systems with neural networks to predict future solar irradiance under different environmental conditions. In [15], a fuzzy clustering method has been proposed to assign days with similar patterns of solar irradiance, thereby improving accuracy rates. The authors of [16] have proposed two probabilistic models based on Bayesian inference for short-term forecasting of PV. Furthermore, a generative deep neural network model has been suggested in [17] for probabilistic spatio-temporal solar irradiance forecasting.

More recently, considerable interest has been directed to develop ensemble forecasting methods. These methods are based on the aggregation of multiple predictors to increase accuracy rates of solar irradiance forecasting. In [18], the authors have proposed a solar generation forecasting method

This work was supported by the Department of Electrical Engineering and Automation, School of Electrical Engineering, Aalto University, Finland.

M. Abdel-Nasser is with the Department of Computer Engineering and Mathematics, University Rovira i Virgili, 43007 Tarragona, Spain, and also with the Department of Electrical Engineering, Aswan University, 81542 Aswan, Egypt (e-mail: mohamed.abdelnasser@urv.cat).

K. Mahmoud is with the Department of Electrical Engineering and Automation, Aalto University, 00076 Espoo, Finland, and also with the Department of Electrical Engineering, Aswan University, 81542 Aswan, Egypt (e-mail: karar.mostafa@allto.fi).

M. Lehtonen is with the Department of Electrical Engineering and Automation, Aalto University, 00076 Espoo, Finland (e-mail: matti.lehtonen@allto.fi).

based on combined cluster analysis and an ensemble model. In [19], an ensemble framework for the day-ahead forecast has been proposed based on five different structures of feedforward neural networks. In [20], [21], ensemble approaches that utilize boosting algorithms have been proposed for short-term solar irradiance forecast. These approaches provide accurate results while avoiding the over-fitting problem. Also, ensemble-based methods of different predictors have been introduced in [22] for the forecasting problem, including the Markov Chain model, Bayesian model, and quantile regression.

In general, ensemble models can significantly improve the accuracy in terms of minimizing forecasting errors compared with individual predictors. However, this improvement can be achieved by adopting 1) accurate individual forecasting models, and 2) an appropriate aggregation strategy. Regarding the aggregation strategies, most related works compute average or weighted average values between the predictions of individual forecasting models. Besides, these works ignore the interaction between the values to be aggregated (e.g., predicted solar irradiance values). Therefore, in the case of solar irradiance forecasting, this presumption may be inconsistent with the real scenario, in which solar irradiance holds intermittent characteristics. These aspects have significant impacts on the reliability of the forecasting results of solar irradiance.

To meet the requirements above-mentioned for achieving reliable forecasting results, in this paper, we propose an ensemble-based forecasting approach based on deep long short-term memory (LSTM) models and Choquet integral based aggregation function. This promising combination has the following merits: 1) LSTM is an efficient deep learning technique for constructing the individual forecasting models because they can model temporal changes in solar irradiance, thanks to their recurrent architecture and memory units, and 2) unlike other aggregation functions (e.g., a weighted average), the Choquet integral can model the interaction between the inputs to be aggregated through a fuzzy measure. Choquet integral is a strong reasoning approach under conditions of uncertainty because it deals with the information from multiple models that may conflict with each other [23]. Indeed, Choquet integral has generalization abilities and it does not require to assume independency of one model from another, and so it can be employed in non-linear problems. On the one hand, if the outputs of forecasting models are dependent, a fuzzy measure is utilized to define a weight on each combination of models, allowing to model the interaction existing among the various individual forecasting models. On the other hand, when the forecasting models are independent, the fuzzy measure is additive, and the Choquet integral agrees with the weighted arithmetic mean technique. Considering the intermittent nature of solar irradiance, Choquet integral may be more suitable for solar irradiance forecasting by synthesizing the individual forecasting results to improve the reliability of forecasting performance. Further, it determines the largest consistency of the results among the conflicting and consistency forecasting results, taking advantage of each individual model.

Most related works compare the performance of different forecasting models and select the one with the top accuracy or average them. However, these approaches do not take into account the relationship between the components and neglect essential information. In turn, the Choquet integral introduces an efficient handling strategy for reliable forecasting considering the high variability of the forecasting results among individual forecasting models. To the best of the authors' knowledge, this is the first paper that proposes the use of Choquet integral and LSTM for solar irradiance forecasting or even time-series forecasting problems in general. Here, we focus on forecasting solar irradiance since it is the dominant factor for PV generation. This forecasting approach does not require complex meteorological instrumentation, and so it is cost-effective. We validate the proposed method using six realistic datasets collected from different sites in Finland in which solar irradiance is intermittent. It worth noting that the proposed forecasting approach has no assumption for the data type, and so it is a promising tool for various forecasting applications in smart grids, e.g., wind power, electricity consumption, electricity prices, and electric vehicle demand forecasting problems.

The main contributions of the paper are listed bellow:

- Proposing a reliable ensemble-based solar irradiance forecasting approach without requiring complex meteorological instrumentation;
- Introducing an effective aggregation technique for individual deep LSTM forecasting models based on the Choquet integral;
- Improving the accuracy of solar irradiance forecasting compared to existing individual and ensemble forecasting models;
- Evaluating the effectiveness of the proposed solar irradiance forecasting approach at different sites in Finland.

The remaining of this manuscript is organized as follows. Sections II and III describe preliminary concepts and the proposed method, respectively. The results and conclusion, as well as future work, are given in Section IV and Section V, respectively.

II. Deep LSTM Forecasting Models

Given a historical solar irradiance dataset for a certain site, we individually train different LSTM models to construct a solar irradiance forecasting model for that site. Assume that we have n LSTM models ($M_1, M_2, \dots M_n$), and x_i is the prediction of LSTM model M_i, we use Choquet integral to aggregate the predictions of LSTM Models. In this section, we substantially describe the LSTM models which are the basic building blocks of the proposed reliable deep forecasting model (RDFM).

A. Basic LSTM unit

An LSTM network [24] can model sequence data and the corresponding target $(x_1, y_1), (x_2, y_2), \dots, (x_m, y_m)$. The LSTM network handles new input $x_i \in R^M$ $\forall$ pair (x_i, y_i) and predicts the target y_i given preceding inputs $x_1, \dots, x_i$. The state of the LSTM comprises two vectors: a hidden state vector $\mathbf{h} \in R^D$ and a cell state vector $\mathbf{c} \in R^D$. Fig. 1 shows the basic unit of LSTM. In includes input, forget, and output gates.

At each time step t the activation vectors of the input gate $i_t \in R^D$, forget gate $f_t \in R^D$, output gate $o_t \in R^D$ and block input $g_t \in R^D$ as follows:

$$\mathbf{i}_t = \sigma\left(\mathbf{W}_i\left[\mathbf{h}_{t-1}, \mathbf{x}_t\right]^T + \mathbf{b}_i\right) \tag{1}$$

$$\mathbf{f}_t = \sigma\left(\mathbf{W}_f\left[\mathbf{h}_{t-1}, \mathbf{x}_t\right]^T + \mathbf{b}_f\right) \tag{2}$$

$$\mathbf{o}_t = \sigma\left(\mathbf{W}_o\left[\mathbf{h}_{t-1}, \mathbf{x}_t\right]^T + \mathbf{b}_o\right) \tag{3}$$

$$\mathbf{g}_t = \tanh\left(\mathbf{W}_g\left[\mathbf{h}_{t-1}, \mathbf{x}_t\right]^T + \mathbf{b}_g\right) \tag{4}$$

where $\mathbf{W}_o = [\mathbf{W}_{oh}; \mathbf{W}_{ox}]$, $\mathbf{W}_i = [\mathbf{W}_{ih}; \mathbf{W}_{ix}]$, $\mathbf{W}_g = [\mathbf{W}_{gh}; \mathbf{W}_{gx}]$, $\mathbf{W}_f = [\mathbf{W}_{fh}; \mathbf{W}_{fx}]$, $\mathbf{W}_{oh}, \mathbf{W}_{ih}, \mathbf{W}_{gh}, \mathbf{W}_{fh} \in R^{D\times D}$ are hidden-to-hidden matrices, $\mathbf{W}_{ox}, \mathbf{W}_{ix}, \mathbf{W}_{gx}, \mathbf{W}_{fx} \in R^{D\times M}$ are input-to-hidden matrices, $b_i, b_f, b_o, b_g \in R^D$ are the bias vectors, $\sigma(x) = 1/1 + e^{-x}$ is logistic sigmoid used as gate activation function, and the hyperbolic tangent $\tanh(x)$ is used as activation function for the block input and output.
After we compute the activation vectors of the gates, the next cell state and hidden state are calculated as follows:

$$\mathbf{c}_t = \mathbf{f}_t \odot \mathbf{c}_{t-1} + \mathbf{i}_t \odot \mathbf{g}_t \tag{5}$$

$$\mathbf{h}_t = \mathbf{o}_t \odot \tanh\left(\mathbf{c}_t\right) \tag{6}$$

where $\odot$ refers to the element-wise product.

B. Solar irradiance forecasting using LSTM models

Solar irradiance forecasting can be phrased as supervised learning. Given a set of solar irradiance measurements $\mathbf{R_l} = \{\mathbf{r_{t1}}, \mathbf{r_{t2}}, \ldots, \mathbf{r_{td}}\}$ collected from site l, we can restructure the data to look like a supervised learning problem, where the forecasted values y can be computed from an input variables x using a mapping function $y = f(x)$. This can be done by using previous time steps as input variables and use the next time step as the output variable:

$$\mathbf{S_l} = \begin{bmatrix}\mathbf{x} & \mathbf{y}\end{bmatrix} \tag{7}$$

in which

$$\mathbf{x} = \begin{bmatrix} r_{t1-LB} & \cdots & r_{t1-1} & r_{t1} \\ r_{t2-LB} & \cdots & r_{t2-1} & r_{t2} \\ \vdots & \vdots & \vdots & \vdots \\ r_{td-LB} & \cdots & r_{td-2} & r_{td-1} \end{bmatrix} \tag{8}$$

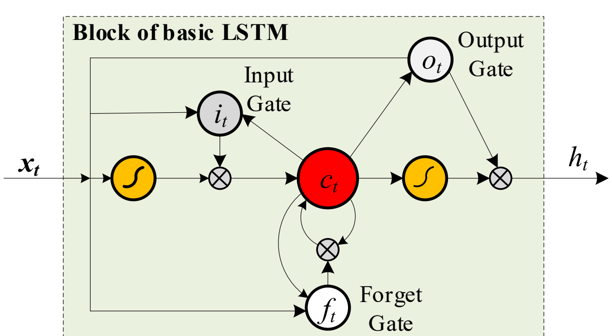

Figure 1. LSTM Cell [25].

$$\mathbf{y} = \begin{bmatrix} r_{t2} \\ r_{t3} \\ \vdots \\ r_{td} \end{bmatrix} \tag{9}$$

Note that at a certain time step, the input variable x can include solar irradiance measurements of several previous time steps, for example, with a look-back of 2, the first row of $\mathbf{S_l}$ can be extend as $x = \{r_{t0}, r_{t1}\}$ with $y = \{r_{t2}\}$. The $\mathbf{S_l}$ matrix of (7) can be transformed to a normalized matrix $\mathbf{z}$ in which each element of raw i and column j can be expressed as follows:

$$z_{ij} = \frac{S_{l,ij} - \min(\mathbf{S_l})}{\max(\mathbf{S_l}) - \min(\mathbf{S_l})} \tag{10}$$

The proposed RDFM receives predictions from individual LSTM models [3]. Each LSTM model learns a different mapping function $f_{M_i}()$ that maps the input variable X to one output variable to be predicted. Below, we explain the architecture of each LSTM forecasting model. In this paper, we use the following four LSTM models.

1) Architecture of Model 1 (M1): Given the solar irradiance at time-step t, our target is to predict the solar irradiance at time $t+1$. M1 is designed as follows: one input, a hidden layer with four LSTM blocks, and an output layer that gives the predicted solar irradiance. This model is trained for a total of 100 epochs with a batch size of 1.

2) Architecture of Model 2 (M2): In this model, we employ multiple recent time-steps to predict solar irradiance at the next time step (a window technique). In this technique, we can tune the size of the window for the solar irradiance forecasting problem. Given the current time t, we aim at predicting the solar irradiance at the next time in the sequence $t+1$. To do so, we use the solar irradiance of the current time t and the ones of two prior times ($t-1$ and $t-2$) as input variables to the LSTM unit. In this case, the input variables of the LSTM unit are the solar irradiance at $t-2$, $t-1$, and t while the output variable is the solar irradiance at $t+1$.

3) Architecture of Model 3 (M3): Indeed, time steps provide another way to phrase the solar irradiance forecasting problem. Like M2, we take previous time steps in the solar irradiance time series as inputs to predict the output power at the next time step. In this model, instead of using the past observations as separate input features, we use them as time steps of the *one input feature*, which is a more accurate framing of the solar irradiance forecasting problem. For instance, if the time step equals 3, the LSTM unit outputs the solar irradiance at t after it handles the solar irradiance at $t-3$, $t-2$ and $t-1$. The main difference between M3 and M2 is the structure of the data fed into each model. Specifically, we use the same data representation of M2 to construct the data for M3, but we set its columns to be the dimension of time steps and set the features dimension to 1.

4) Architecture of Model 4 (M4): In this model, we stack LSTM layers on top of each other in a similar way of the traditional neural networks [26]. The first layer receives the solar radiance values $x_t, x_{t+1}, \ldots x_N$, and the hidden vector h_i is inputted to the next top layer. The hidden states of all the layers are computed from the bottom layer to the top one. The stacked LSTM network can be expressed as follows:

$$h_t^{(l)} = \phi_h \left(W_l^T h_{t-1}^{(l)} + U_l^T h_t^{(l-1)} \right) \tag{11}$$

where ϕ is a nonlinear function, and $h_t^{(l)}$ is the hidden state of the l^{th} layer at time step t. In the case of the first layer, $l = 1$ and thus $h_t^{(l-1)} = x_t$ in this case.

The LSTM models used in this paper have been used in existing studies of solar irradiance and PV power forecasting [3], [27], [28]. Based on these studies, the high performance of LSTM models has been demonstrated.

III. Aggregation function based on Choquet integral

In general, the performance of an individual forecasting model, to some extent, depends on the pattern characteristics of data, and each model has its own uncertainty. Aggregation of information is the process of combining different pieces of information provided by several sources to obtain a unified decision. Unlike the individual models, the aggregation of multiple forecasting models can reduce the variance of forecasting errors and enhance the forecasting results. The aggregation function aggregates n-tuples values belonging to a particular set, into a value of the same set [29]. An aggregation operator is a function that specifies a real number y to n-tuple of real numbers $(x_1, x_2, \ldots, x_n)$:

$$y = \alpha\left(x_1, x_2, \ldots, x_n\right) \tag{12}$$

Definition III.1. An n-tuple function $\alpha : [0, 1]^n \to [0, 1]$ is an aggregation function, if and only if, the following properties are satisfied:

- *Identity:* $\alpha(x) = x$.
- *Boundary conditions:* $\alpha(0_1, ..., 0_n) = 0$ and $\alpha(1_1, ..., 1_n) = 1$.
- *Monotonicity:* If $x_i \leq y_i \ \forall \ i \in \{1, \ldots, n\}$ then $\alpha(x_1, ..., x_n) \leq \alpha(y_1, ..., y_n)$.

Common examples of the aggregation functions are the maximum function ($\alpha(x) = \max\{x_1, \ldots, x_n\}$), the minimum function ($\alpha(x) = \min\{x_1, \ldots, x_n\}$) and the arithmetic mean function ($\alpha(x) = 1/n \sum_i^n \{x_1, \ldots, x_n\}$).

In this paper, we use the Choquet integral that is formed based on a fuzzy measure. A fuzzy measure represents the degree of relationship between the elements to be aggregated. Choquet integral regards the relevance of each component to be aggregated and its interactions with other items.

Definition III.2. Let $Q = \{1, \ldots, n\}$ be a reference set, and 2^Q be the power set of Q. A function $\mu : 2^Q \to [0, 1]$ is said to be fuzzy measure if it fulfills the following properties $\forall \ A, B \subseteq Q$:

- *Boundary condition:* $\mu(\emptyset) = 0, \ \mu(X) = 1$.
- *Monotonicity:* If $A \subseteq B$ then $\mu(A) \leq \mu(B)$.

Definition III.3. The discrete Choquet integral $\chi : [0, 1]^n \to [0, 1]$ of n-tuple of real numbers $x = (x_1, x_2, \ldots, x_n)$ wrt. a fuzzy measure $\mu : 2^Q \to [0, 1]$, can be defined as follows:

$$\chi_\mu(x) = \sum_{i=1}^{n} (x_{(i)} - x_{(i-1)}) \cdot \mu(A_{(i)}), \tag{13}$$

An increasing permutation is applied on $x = (x_1, x_2, \ldots, x_n)$ to get $(x_{(1)}, x_{(2)}, \ldots x_{(n)})$, in which $_{(i)}$ refers to an index $i = \{1, 2, \ldots, n\}$, and thus $0 \leq x_{(1)} \leq x_{(2)} \leq \ldots \leq x_{(n)}$, $x_{(0)} = 0$, and $A_i = \{x_{(i)}, \ldots, x_{(n)}\}$ are the indices of $n-i+1$ largest element of x.

As we can see, $\chi_\mu(x)$ fulfills the properties of aggregation functions (Definition III.1). The Choquet integral $\chi_\mu(x)$ can be also expressed as follows:

$$\chi_\mu(x) = \sum_{i=1}^{n} (x_{(i)} \cdot \mu(A_{(i)}) - x_{(i-1)} \cdot \mu(A_{(i)})) \tag{14}$$

Regarding the fuzzy measure, in this work, we adopt the power measure defined as the power mean of the cardinality of the set of values aggregated. This fuzzy measure $\mu_{pm} : 2^N \to [0, 1]$ is defined as follows:

$$\mu_{pm}(A) = (\frac{|A|}{n})^q \quad \text{with } q > 0 \tag{15}$$

We use the grey wolf optimizer (GWO) [30] to determine the best value for q, finding that the best value is 2. Note that any other evolutionary algorithm can be employed for this purpose. Fig. 2 shows the proposed aggregation procedure of various LSTMs using the Choquet integral. Unlike other aggregation functions, the main feature of the Choquet integral is that it considers, through the fuzzy measure, the interaction between the components when aggregating them. For example, the maximum does not take into account the relationship between the components and neglects essential information. The Choquet integral can represent wide expressive capabilities and model various aggregation operators, such as the weighted sum, the minimum, maximum, and ordered weighted average. Fuzzy measure can be considered as the degree of subjective importance of various individual forecasting models in the aggregation process. For this reason, the application of Choquet integral introduces an efficient handling strategy for reliable forecasting considering the high variability of the forecasting results of individual forecasting models.

IV. Implementation of RDFM using Choquet Integral and Deep LSTMs

In the training phase, we rephrase the dataset of each site S_l as described in (7), and then train the LSTM model M_i to get a mapping function $f_{M_i}()$ for this model. At a time step t, the predicted solar irradiance value y_t using the LSTM model M_i is calculated as follows: $y_t = f_{M_i}(x_t)$. For n LSTM models, we obtain n predicted solar irradiance values by feeding x_t into the learned mapping functions:

$$r_l = \{f_{M_1}(x_t), f_{M_2}(x_t), \ldots, f_{M_n}(x_t)\} \tag{16}$$

In Algorithm 1 we describe the steps to implement RDFM. In the testing phase, the predicted solar irradiance values r_l are aggregated using Choquet integral expressed by (14). Note that the aggregation function (14) requires the computation of μ_{pm} given in (15), in which the parameter q has previously been obtained using the validation set.

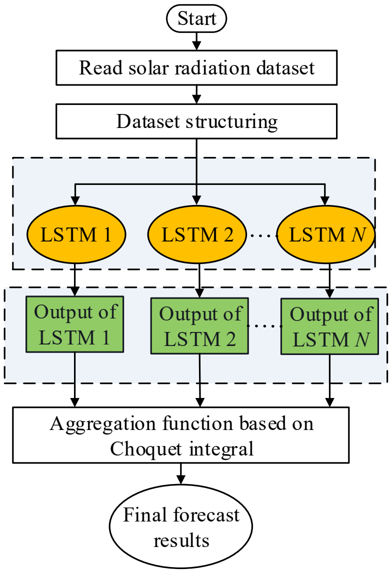

Figure 2. Proposed aggregation using Choquet integral.

Algorithm 1 Implementation of RDFM

Read historical data (solar irradiance) of all sites.
Structure the data by splitting them into training, validation, and testing sets.
Rearrange the data using for all sites using (7), and normalize them using (10).
while $i \leq n$ **do**
    Train the LSTM model i (i.e., M_i)
    Save the LSTM model i
    $i = i + 1$
end
    while true **do**
        Read S_l, M1, M2, M3, M4, q
        foreach time step t **do**
            Compute $f_{M_1}(x_t), f_{M_2}(x_t), f_{M_3}(x_t), f_{M_4}(x_t)$
            $r_l \leftarrow \{r1, r2, r3, r4\}$
            Permute r_l increasingly
            Compute $\mu_{pm}(A)$ using (15)
            Aggregate r_l using (14)
            Forecast value$\leftarrow \chi_{\mu}^{\kappa}$
    end

To assess the accuracy of the forecasting models, root mean square error (RMSE) is calculated, which can be formulated as follows:

$$RMSE = \sqrt{\frac{1}{N}\sum_{i=1}^{N}\left(R_{\text{predicted},i} - R_{\text{observed},i}\right)^2} \tag{17}$$

where $R_{predicted}$ and $R_{observed}$ are the predicted and observed values of solar irradiance, respectively.

V. Results and discussion

A. Finland Solar Irradiance Datasets

In this paper, we use realistic datasets for solar irradiance in Finland to assess the performance of the proposed method.

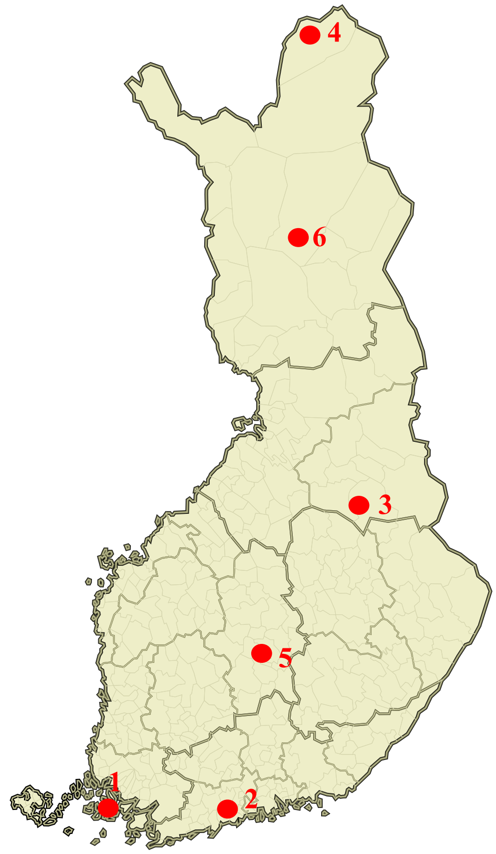

Figure 3. The sites where solar irradiance are measured in Finland.

Table I
RMSE of the proposed RDFM and 4 deep LSTM models

Model	Site 1	Site 2	Site 3	Site 4	Site 5	Site 6
M1	31.05	34.91	37.15	23.58	36.61	23.21
M2	30.24	34.98	35.00	23.50	35.84	23.27
M3	34.14	31.30	33.83	26.52	30.74	24.36
M4	34.23	36.55	36.70	24.63	38.51	29.13
RDFM	**26.71**	**30.33**	**29.88**	**20.77**	**30.20**	**19.72**

These datasets are collected from the Finnish meteorological institute [31]. The datasets involve measured global solar irradiance for a whole year with a 1-hour resolution for different six sites in Finland. Here, global solar irradiance refers to the horizontal plane. Fig. 3 shows the six sites (sites 1, 2, 3, 4, 5, 6) represented by red dots on the map of Finland where solar irradiance is collected. As noticed, these sites are distributed from the north to the south of Finland, where each site can represent a different climate zone.

To show the variability of the datasets, in Fig. 4 we provide the distribution of solar irradiance at sites 1 and 4, which are located in two away areas. Specifically, we present the distribution of solar irradiance in datasets with (a,d) hours, (b,e) days, and (c,f) samples. The first and second rows represent the distributions of datasets of sites 1 and 4, respectively. Fig. 4 (a) shows that the maximum solar irradiance at site 4 during the day where it is noticed at 12:00 o'clock; however, it is at 13:00 o'clock at site 1 (based on the median values for each

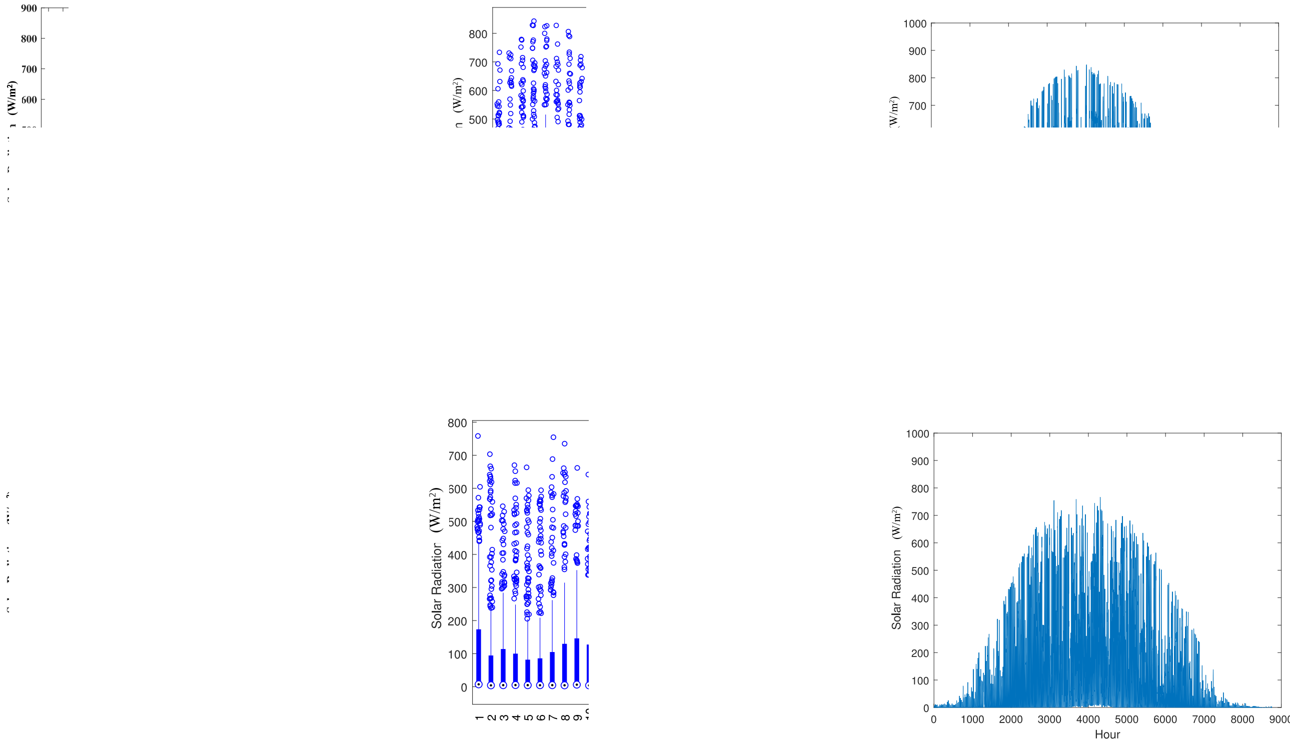

(f)

Figure 4. The distribution of solar irradiance in datasets with (a,d) hours, (b,e) days, and (c,f) samples. The first and second rows represent the distributions of datasets of sites 1 and 4, respectively.

Table II
RMSE OF THE PROPOSED RDFM AND 4 DEEP LSTM MODELS WITH THREE DIFFERENT SOLAR PROFILES (SP1, SP2 AND SP3)

Model	RDFM			M1			M2			M3			M4		
Profile	SP1	SP2	SP3	SP1	SP2	SP3	SP1	SP2	SP3	SP1	SP2	SP3	SP1	SP2	SP3
Site 1	23.19	60.03	50.36	25.79	63.98	51.35	23.78	71.32	51.33	178.73	176.95	103.66	25.44	62.23	53.27
Site 2	37.69	62.05	39.32	42.78	72.12	47.91	43.29	63.85	47.76	38.51	59.33	42.36	42.33	58.32	45.46
Site 3	32.49	67.60	56.09	44.30	81.92	64.61	40.95	73.54	59.92	36.72	68.99	40.79	64.57	63.94	47.78
Site 4	23.98	47.75	40.41	29.07	56.09	29.67	28.06	55.92	28.91	23.72	49.54	33.93	23.76	49.94	29.52
Site 5	20.07	59.46	38.24	26.93	75.02	37.10	26.73	72.63	37.57	20.02	61.09	37.29	19.55	63.30	33.11
Site 6	17.95	37.22	20.48	25.77	45.15	27.16	26.53	49.23	27.25	22.17	44.93	25.42	22.09	44.38	25.42

hour), as shown in Fig. 4 (d). Another difference is that the solar irradiance at site 1 has a higher trend than those of site 4 (see Fig. 4 (b, e, c, f)). Interestingly, the solar irradiance at the beginning of the year follows an increasing trend until the mid-year where it starts to decrease. This figure illustrates the difference between the solar radiation at different sites in Finland. This high variability associated with the Finnish solar irradiance profile requires a reliable forecasting method to represent such intermittent and fluctuating features accurately.

B. Performance of the Forecasting Models

In this study, we split each solar irradiance dataset into training, validation and testing ones (70% for training, 15% validation and 15% testing). The time step for RDFM is 1 hour. Table I compares the values of RMSE for the four LSTM models (M1, M2, M3, and M4) and RDFM. As we can see, the RMSE values of RDFM are much lower than those of the other individual LSTM models for all sites. For instance, M1, M2, M3, and M4 achieve RMSE values of 31.05, 30.24, 34.14, 34.23, respectively, with the data of site 1. However, the proposed RDFM yields only an RMSE value of 26.71 with the data of the same site. We also notice similar reductions in the RMSE values in the other five sites.

To visualize the performance of forecasting models, in Fig. 5 we compare the predicted solar irradiance obtained by the five forecasting models with the actual solar irradiance values of the six sites for seven days (one week). The individual four LSTM models deliver accurate prediction results, and thus we fulfill the first requirement for achieving a reliable forecasting model (i.e., selecting accurate individual forecasting models). Yet, the RDFM gives more accurate predictions for the different solar irradiance profiles. Fig. 5 demonstrates that the four

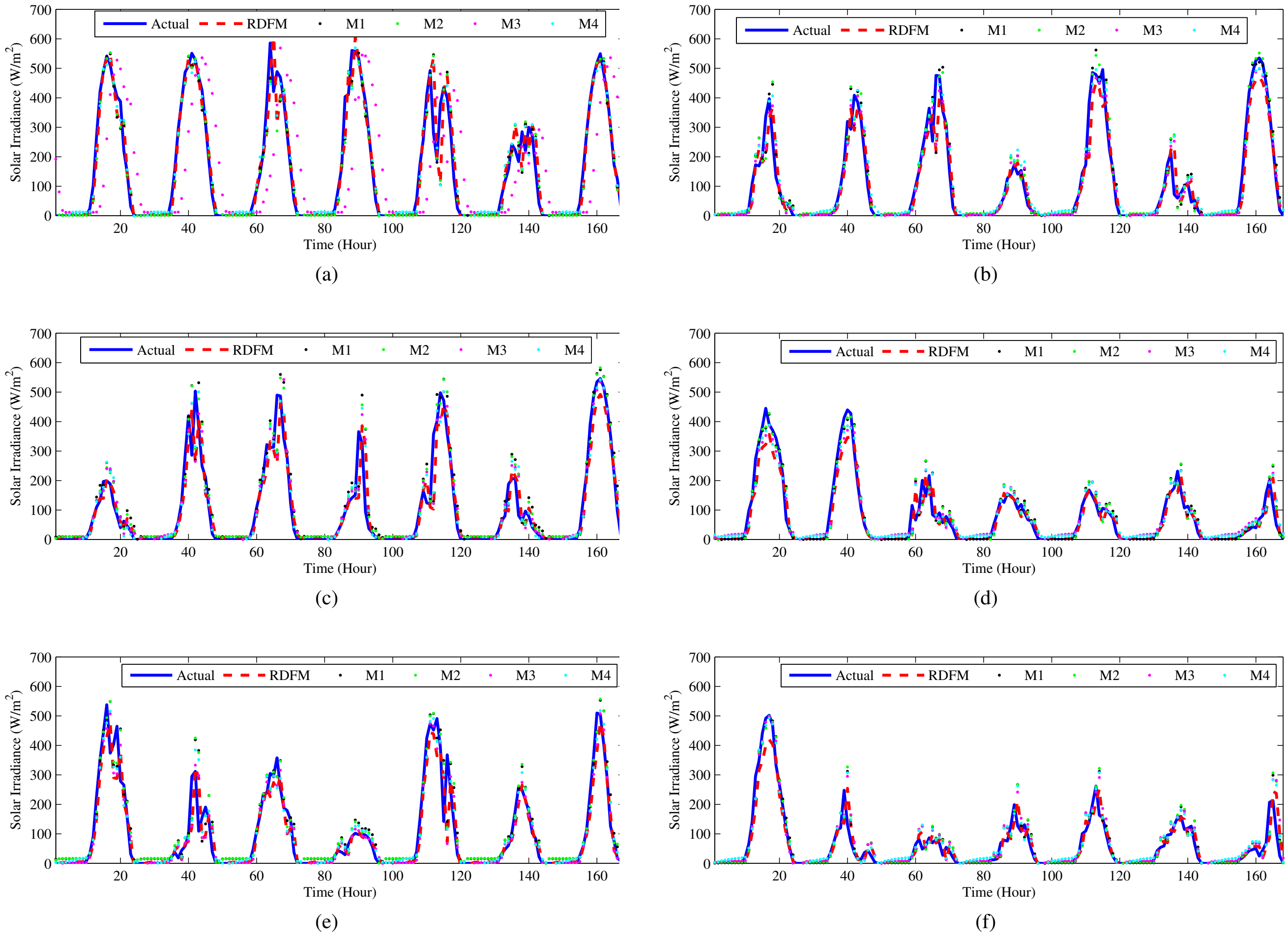

Figure 5. The predicted solar irradiance with RDFM for (a) Site 1, (b) Site 2, (c) Site 3, (d) Site 4, (e) Site 5, and (f) Site 6.

LSTM models (represented by dots) often overestimate or underestimate the solar irradiance values while RDFM achieves higher matching concerning the actual values, thanks to the Choquet integral based aggregation approach that can model the interaction between the predicted values of the individual LSTM models through the fuzzy measure. The reductions achieved with the aggregation approach implies that we fulfill the second requirement for achieving a reliable forecasting model (i.e., selecting appropriate aggregation function). This analysis reveals the reliability of the proposed model since its prediction results are much accurate than the ones of the individual models at all sites.

C. Performance of Forecasting Models with Different Solar Irradiance profiles

Solar irradiance can have highly fluctuating daily profiles. Here, we evaluate the forecasting models with different solar irradiance daily profiles. This observation implies that the accuracy of forecasting models increases with the clearness index. From now on, we refer to clear, cloudy, and partially cloudy profiles as SP1, SP2, and SP3, respectively. We identify these three profiles according to the clearance index given in [32]. In Table II, we compare the RMSE values of the proposed RDFM and four deep LSTM models with the three different solar irradiance profiles. In general, the proposed RDFM yields the lowest forecasting errors at the six sites for the three solar irradiance profiles. Another important notice is that the lowest and highest forecasting errors for M1, M2, M3, and M4 at the six sites are founded with SP1 and SP3, respectively. However, the proposed RDFM shows lower errors even with low clearness index values, i.e., highly fluctuated days. This comparison reveals the high reliability of the proposed forecasting model with different sites and solar profiles. Consequently, RDFM is a suitable tool for forecasting the high fluctuating solar irradiance in Finland, thanks to the Choquet integral based aggregation method that properly combines the predictions of the individual LSTM models. Regarding the case when applying the proposed approach to data referring to different seasons, it is expected that the proposed approach will give similar performance compared to the existing approaches.

D. Comparisons

Here, we compare the accuracy of the proposed RDFM with two individual forecasting methods (persistence and ARIMA) and 4 ensemble forecasting methods. Specifically, we compare

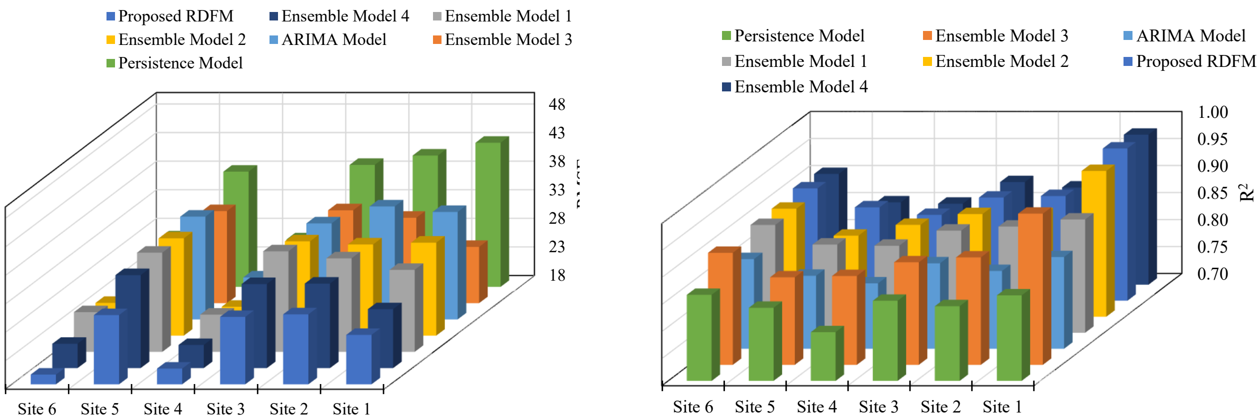

(a) (b)

Figure 6. Performance evaluation of the proposed RDFM approach against different forecasting models. (a) RMSE and (b) R^2 evaluation metrics.

RDFM with four ensemble integration techniques: the average ensemble (Ensemble Model 1) [33], the weighted average ensemble (Ensemble Model 2) proposed in [34], the median ensemble (Ensemble Model 3) [35], and ensemble of deep three LSTM models and ARIMA (Ensemble Model 4). It worth noting that Ensemble Model 4 is a variant of the proposed approach, but we replace M4 with ARIMA.

In Fig. 6(a,b), we compare the RMSE and R^2 (coefficient of determination) values of the proposed model against the two individual forecasting methods (ARIMA and persistence) as well as the four ensemble strategies. The highest RMSE values are noticed with the persistence method at all sites while the lowest R^2 values are noticed in the same method. This trend implies that the persistence method has the worst accuracy rate compared to the other forecasting methods and the proposed method. ARIMA obtains better performance that the persistence model for all sites. In turn, Ensemble Models 1, 2 and 3 achieve better forecasting results than the ARIMA and persistence methods. Ensemble Model 4 yields a better forecasting results compared to Ensemble Models 1, 2 and 3, thanks to the Choquet integral. Obviously, the proposed RDFM outperforms the compared ensemble aggregation strategies as well as the individual forecasting methods for all sites. The superiority of the proposed RDFM is justified by the high accuracy of the 4 individual LSTM models and the effectiveness of the Choquet integral.

VI. Conclusions

In this paper, we have proposed a reliable forecasting method based on LSTM models aggregated by Choquet integral, which can inherit advantages of the individual models and avoids their disadvantage. The individual LSTM models achieve accurate predictions because they can model the temporal changes in solar irradiance while the Choquet integral can model the interaction between the predictions of individual models through the fuzzy measure. Most related works compare the performance of different forecasting models and select the one of the highest accuracy or average them. However, these approaches do not take into account the relationship between the components and neglect inherent information. In turn, Choquet integral introduces an efficient handling strategy for reliable forecasting by considering the high variability of the forecasting results of individual forecasting models. To validate the proposed approach, we have applied it to forecast solar irradiance at six sites in Finland. Furthermore, we have compared it with different individual and ensemble-based forecasting approaches. The proposed forecasting approach has shown lower forecasting errors than the other methods, even with highly fluctuated solar irradiance profiles.

Notably, the proposed approach has no assumption for the data type, and thus it can be a sufficient tool for diverse forecasting problems in smart grids (wind power, electricity consumption, etc.). An economic impact of the proposed approach is that the complex meteorological instrumentation is inessential. However, whenever local weather stations are available, such further weather measurements (e.g. wind speed, cloud cover, and temperature) can be fed into the proposed RDFM. In the future, we will integrate the forecasting model with predictive management in smart grids.

References

[1] V. Quaschning, *Understanding renewable energy systems*. Routledge, 2016.

[2] V. Khare, S. Nema, and P. Baredar, "Solar–wind hybrid renewable energy system: A review," *Renewable and Sustainable Energy Reviews*, vol. 58, pp. 23–33, 2016.

[3] M. Abdel-Nasser and K. Mahmoud, "Accurate photovoltaic power forecasting models using deep lstm-rnn," *Neural Computing and Applications*, pp. 1–14, 2017.

[4] X. Yang, M. Xu, S. Xu, and X. Han, "Day-ahead forecasting of photovoltaic output power with similar cloud space fusion based on incomplete historical data mining," *Applied Energy*, vol. 206, pp. 683–696, 2017.

[5] M. Ceci, R. Corizzo, F. Fumarola, D. Malerba, and A. Rashkovska, "Predictive modeling of pv energy production: How to set up the learning task for a better prediction?" *IEEE Transactions on Industrial Informatics*, vol. 13, no. 3, pp. 956–966, 2016.

[6] D. W. Van der Meer, J. Widén, and J. Munkhammar, "Review on probabilistic forecasting of photovoltaic power production and electricity consumption," *Renewable and Sustainable Energy Reviews*, vol. 81, pp. 1484–1512, 2018.

[7] G. Capizzi, C. Napoli, and F. Bonanno, "Innovative second-generation wavelets construction with recurrent neural networks for solar radiation forecasting," *IEEE Transactions on neural networks and learning systems*, vol. 23, no. 11, pp. 1805–1815, 2012.

[8] S. Salcedo-Sanz, C. Casanova-Mateo, A. Pastor-Sánchez, and M. Sánchez-Girón, "Daily global solar radiation prediction based on a hybrid coral reefs optimization–extreme learning machine approach," *Solar Energy*, vol. 105, pp. 91–98, 2014.

[9] L. Benali, G. Notton, A. Fouilloy, C. Voyant, and R. Dizene, "Solar radiation forecasting using artificial neural network and random forest methods: Application to normal beam, horizontal diffuse and global components," *Renewable energy*, vol. 132, pp. 871–884, 2019.

[10] R. Prasad, M. Ali, P. Kwan, and H. Khan, "Designing a multi-stage multivariate empirical mode decomposition coupled with ant colony optimization and random forest model to forecast monthly solar radiation," *Applied energy*, vol. 236, pp. 778–792, 2019.

[11] F. Golestaneh, P. Pinson, and H. B. Gooi, "Very short-term nonparametric probabilistic forecasting of renewable energy generation—with application to solar energy," *IEEE Transactions on Power Systems*, vol. 31, no. 5, pp. 3850–3863, 2016.

[12] C. Wan, J. Lin, Y. Song, Z. Xu, and G. Yang, "Probabilistic forecasting of photovoltaic generation: An efficient statistical approach," *IEEE Transactions on Power Systems*, vol. 32, no. 3, pp. 2471–2472, 2016.

[13] K. B. Debnath and M. Mourshed, "Forecasting methods in energy planning models," *Renewable and Sustainable Energy Reviews*, vol. 88, pp. 297–325, 2018.

[14] S. Chen, H. Gooi, and M. Wang, "Solar radiation forecast based on fuzzy logic and neural networks," *Renewable Energy*, vol. 60, pp. 195–201, 2013.

[15] P. Luo, S. Zhu, L. Han, and Q. Chen, "Short-term photovoltaic generation forecasting based on similar day selection and extreme learning machine," in *2017 IEEE Power & Energy Society General Meeting*. IEEE, 2017, pp. 1–5.

[16] A. Bracale, G. Carpinelli, P. De Falco, R. Rizzo, and A. Russo, "New advanced method and cost-based indices applied to probabilistic forecasting of photovoltaic generation," *Journal of Renewable and Sustainable Energy*, vol. 8, no. 2, p. 023505, 2016.

[17] M. Khodayar, S. Mohammadi, M. E. Khodayar, J. Wang, and G. Liu, "Convolutional graph autoencoder: A generative deep neural network for probabilistic spatio-temporal solar irradiance forecasting," *IEEE Transactions on Sustainable Energy*, pp. 1–1, 2019.

[18] C. Pan and J. Tan, "Day-ahead hourly forecasting of solar generation based on cluster analysis and ensemble model," *IEEE Access*, vol. 7, pp. 112 921–112 930, 2019.

[19] M. Q. Raza, M. Nadarajah, J. Li, K. Y. Lee, and H. B. Gooi, "An ensemble framework for day-ahead forecast of pv output in smart grids," *IEEE Transactions on Industrial Informatics*, 2018.

[20] J. Wang, P. Li, R. Ran, Y. Che, and Y. Zhou, "A short-term photovoltaic power prediction model based on the gradient boost decision tree," *Applied Sciences*, vol. 8, no. 5, 2018. [Online]. Available: https://www.mdpi.com/2076-3417/8/5/689

[21] S. Tiwari, R. Sabzehgar, and M. Rasouli, "Short term solar irradiance forecast using numerical weather prediction (nwp) with gradient boost regression," in *2018 9th IEEE International Symposium on Power Electronics for Distributed Generation Systems (PEDG)*. IEEE, 2018, pp. 1–8.

[22] A. Bracale, G. Carpinelli, and P. De Falco, "A probabilistic competitive ensemble method for short-term photovoltaic power forecasting," *IEEE Transactions on Sustainable Energy*, vol. 8, no. 2, pp. 551–560, 2016.

[23] Y. Cao, "Aggregating multiple classification results using choquet integral for financial distress early warning," *Expert Systems with Applications*, vol. 39, no. 2, pp. 1830–1836, 2012.

[24] K. Greff, R. K. Srivastava, J. Koutník, B. R. Steunebrink, and J. Schmidhuber, "Lstm: A search space odyssey," *IEEE transactions on neural networks and learning systems*, vol. 28, no. 10, pp. 2222–2232, 2016.

[25] A. Graves, A.-r. Mohamed, and G. Hinton, "Speech recognition with deep recurrent neural networks," in *2013 IEEE international conference on acoustics, speech and signal processing*. IEEE, 2013, pp. 6645–6649.

[26] R. Pascanu, C. Gulcehre, K. Cho, and Y. Bengio, "How to construct deep recurrent neural networks," in *Proceedings of the Second International Conference on Learning Representations (ICLR 2014)*, 2014.

[27] Y. Yu, J. Cao, and J. Zhu, "An lstm short-term solar irradiance forecasting under complicated weather conditions," *IEEE Access*, vol. 7, pp. 145 651–145 666, 2019.

[28] X. Qing and Y. Niu, "Hourly day-ahead solar irradiance prediction using weather forecasts by lstm," *Energy*, vol. 148, pp. 461–468, 2018.

[29] J. C. S. Bueno, C. A. Dias, G. P. Dimuro, H. Santos, E. N. Borges, G. Lucca, and H. Bustince, "Aggregation functions based on the choquet integral applied to image resizing," in *2019 Conference of the International Fuzzy Systems Association and the European Society for Fuzzy Logic and Technology (EUSFLAT 2019)*. Atlantis Press, 2019.

[30] K. Mahmoud, M. M. Hussein, M. Abdel-Nasser, and M. Lehtonen, "Optimal voltage control in distribution systems with intermittent pv using multiobjective grey-wolf-lévy optimizer," *IEEE Systems Journal*, 2019.

[31] "Finnish meteorological institute," Accessed: 01-07-2019. [Online]. Available: https://en.ilmatieteenlaitos.fi/

[32] S. Leva, A. Dolara, F. Grimaccia, M. Mussetta, and E. Ogliari, "Analysis and validation of 24 hours ahead neural network forecasting of photovoltaic output power," *Mathematics and computers in simulation*, vol. 131, pp. 88–100, 2017.

[33] S. Borovkova and I. Tsiamas, "An ensemble of lstm neural networks for high-frequency stock market classification," *Journal of Forecasting*, 2019.

[34] Q. Ni, S. Zhuang, H. Sheng, G. Kang, and J. Xiao, "An ensemble prediction intervals approach for short-term pv power forecasting," *Solar Energy*, vol. 155, pp. 1072–1083, 2017.

[35] M. H. Alobaidi, P. R. Marpu, T. B. Ouarda, and H. Ghedira, "Mapping of the solar irradiance in the uae using advanced artificial neural network ensemble," *IEEE Journal of Selected Topics in Applied Earth Observations and Remote Sensing*, vol. 7, no. 8, pp. 3668–3680, 2014.

Mohamed Abdel-Nasser received the Ph.D. degree in Computer Engineering from the University Rovira i Virgili (URV) in 2016. He has been a postdoc researcher at the URV since 2018, and Assistant Professor at the Electrical Engineering Department, Aswan University (Egypt) since 2016. In 2017, he has received the Marc Esteva Vivanco prize for the best Ph.D. dissertation on Artificial Intelligence. He has participated in several projects funded by the European Union and the Government of Spain. He has published more than 60 papers in international journals and conferences. He was the manager of the E-learning & digital library center at Aswan University (2018). His research interests include the application of machine learning and deep learning to several real-world problems, including smart grid analysis, time-series forecasting, and medical image analysis.

Karar Mahmoud received the Ph.D. degree from the Electric Power and Energy System Laboratory (EPESL), Graduate School of Engineering, Hiroshima University, Hiroshima, Japan, in 2016. Since 2010, he has been with Aswan University (Egypt), where he is presently an Assistant Professor. He is currently a Postdoctoral Researcher with the School of Electrical Engineering, Aalto University, Finland. He has authored or coauthored more than 58 publications in top-ranked journals (including 9 IEEE journals), international conferences, and book chapters. His research interests include power systems, renewable energy sources, smart grids, distributed generation, electric vehicles, distributed system management, optimization, and applied machine/deep learning.

Matti Lehtonen received the M.Sc. and Licentiate degrees in electrical engineering from the School of Electrical Engineering, Aalto University (formerly Helsinki University of Technology), Espoo, Finland, in 1984 and 1989, respectively, and the D.Sc. degree from the Tampere University of Technology, Tampere, Finland, in 1992. Since 1987, he has been with VTT Energy, Espoo, Finland, and since 1999, he has been with the School of Electrical Engineering, Aalto University, where he is currently the Head of Power Systems and High Voltage Engineering Department. His research interests include earth fault problems, and harmonic-related issues and applications of information technology in distribution automation and distribution energy management.